water

MDPI

Communication

Synergistic Piezo-Catalytic Inactivation of Bacteria by Dual-Frequency Ultrasound (120 + 1700 kHz) Using Persulfate and ZnO Nano- and Microparticles

Irina Tsenter [1], Elena Kobunova [1,2], Galina Matafonova [1,*] and Valeriy Batoev [1]

[1] Laboratory of Engineering Ecology, Baikal Institute of Nature Management SB RAS, 670047 Ulan-Ude, Russia
[2] Chemistry Faculty, Buryat State University, 670000 Ulan-Ude, Russia
* Correspondence: ngal@binm.ru

Abstract: Dual-frequency ultrasound (DFUS) coupled with sonocatalysts has emerged to be an advanced tool for antimicrobial applications in medicine but remains scarcely studied for water disinfection. In the present work, we first integrated high-frequency DFUS (120 + 1700 kHz), persulfate ($S_2O_8^{2-}$) and ZnO nano- (50 nm) and microparticles (1 µm) for eradicating *Escherichia coli* and *Enterococcus faecalis* in synthetic water. For *E. coli*, the efficiency of DFUS-based processes can be ranked as follows: DFUS < DFUS/ZnO < DFUS/$S_2O_8^{2-}$ < DFUS/ZnO/$S_2O_8^{2-}$. A similar efficiency of the DFUS/$S_2O_8^{2-}$ and DFUS/ZnO/$S_2O_8^{2-}$ processes was found for more resistant *E. faecalis*. In the absence of persulfate, the performance of 1 µm ZnO was higher than that observed with 50 nm for inactivating *E. coli* via the DFUS/ZnO and 1700 kHz/ZnO processes. A synergy of DFUS in terms of 5-log (total) reduction was found in the $S_2O_8^{2-}$/ZnO-based systems, being higher for *E. faecalis* (synergistic coefficient = 1.8–3.0). The synergistic effect was proposed to be driven by the boosted generation of reactive oxygen species and sonoporation. This study opens prospects for the development of novel DFUS-based piezo-catalytic systems for efficient water disinfection.

Keywords: dual-frequency ultrasound; 120 kHz; 1700 kHz; synergistic effect; zinc oxide; persulfate; piezo-catalysis; microbial inactivation

Citation: Tsenter, I.; Kobunova, E.; Matafonova, G.; Batoev, V. Synergistic Piezo-Catalytic Inactivation of Bacteria by Dual-Frequency Ultrasound (120 + 1700 kHz) Using Persulfate and ZnO Nano- and Microparticles. *Water* **2023**, *15*, 2937. https://doi.org/10.3390/w15162937

Academic Editors: Andrea G. Capodaglio, Weiying Feng, Fang Yang and Jing Liu

Received: 7 July 2023
Revised: 4 August 2023
Accepted: 10 August 2023
Published: 15 August 2023

1. Introduction

Environmentally safe, effective and rapid water disinfection remains an up-to-date problem in view of limited drinking water supply in many parts of the world. Ultrasonication is known as an efficient green method for inactivating pathogenic microorganisms in water using reactive oxygen species (ROS), such as hydroxyl radicals (•OH). These are produced from the collapse of microbubbles during acoustic cavitation and the sonoactivated catalysts/oxidants if used. The latter refers to ultrasound-based advanced oxidation processes (US-AOPs), such as semiconductor sonocatalysis and sonophotocatalysis, which are regarded as powerful tools for water treatment and disinfection due to boosted ROS generation and hence shortened exposure times and reduced energy requirements [1–5]. It is important to emphasize that previous research on microbial inactivation in aqueous media by US-AOPs dealt mainly with single-frequency ultrasound.

The other way of improving the performance of ultrasonication is simultaneous exposure to two or more frequencies. This may lead to synergy in terms of increased inactivation efficiency (rate), which is higher than the sum of that obtained under single frequencies. In our review, dual-frequency ultrasonication coupled with catalysts/oxidants, i.e., DFUS-AOPs, has been identified as a promising strategy for water disinfection [6]. Unlike the degradation of organic contaminants, the inactivation of microbial pathogens in water by DFUS-AOPs is still poorly studied. So far, DFUS at low frequencies (≤100 kHz) was employed for water disinfection in pairs of 16 + 20 kHz [7], 17 + 33 and 70 + 100 kHz combined with NaClO [8,9]. Nonetheless, DFUS at high frequencies (>100 kHz up to 2.4 MHz)

was successfully used over the last decade in medical research on sonodynamic therapy (SDT) and sonoantimicrobial chemotherapy [10–14]. Briefly, SDT induces the apoptosis of target (tumor) cells by ROS, which are generated upon the ultrasonic excitation of organic and inorganic sonosensitizers. Historically, organic sonosensitizers, such as porphyrins and xanthones, were derived from SDT. Inorganic sonosensitizers (piezo-catalysts), primarily modified TiO_2 and ZnO and their composites, have wider applications and also showed a high efficiency for microbial inactivation via single-frequency sonocatalysis in the low-frequency range of 20–48 kHz [15–17]. Meanwhile, recent single-frequency SDT studies have confirmed the high efficiency of modified TiO_2- and ZnO-based catalysts upon excitation with a high frequency of 1 MHz [18–22]. Regarding dual-frequency SDT research, only Ninomiya et al. (2014) [23] reported enhanced •OH production by the simultaneous application of DFUS (0.5 + 1 MHz) and TiO_2 nanoparticles modified with targeting protein. Given the promising results of SDT, we consider integrating high-frequency DFUS and inorganic sonocatalysts as a novel hybrid DFUS-AOP for improved water disinfection.

ZnO represents a bio- and eco-friendly, stable and low-cost product with numerous applications. It is known that ZnO exhibits high piezoelectric properties due to its noncentrosymmetric crystal structure [24]. This means that under the action of mechanical forces, the electric charge (electron and holes that move in opposite directions) appears on the crystals [25]; therefore, under exposure to ultrasonic waves in aqueous media, the occurred electric charge changes with the same frequency. Electrons and holes react with O_2 and H_2O with the generation of ROS, such as $\bullet O_2^-$, •OH and H_2O_2, via a known mechanism for piezoelectric catalysts [26]. The generated ROS facilitate lipid peroxidation that affects membrane structure and fluidity and leads to significant damage to membrane proteins [27]. As such, piezo-catalytic disinfection over the last few years has emerged as a highly efficient and inexpensive technology [28]. Recently, Li et al. (2023) [29] comprehensively surveyed the mechanisms of piezoelectric effect-mediated catalysis with different piezoelectric materials and their applications in environmental pollution remediation, including water disinfection. •OH was found to be the main oxidation species under exposure to 38 and 80 kHz in the presence of ZnO [30], whereas $\bullet O_2^-$ and •OH were primarily generated by the 1 MHz + ZnO process [31]. ZnO-based composites, such as Bi_2O_3-ZnO-B_2O_3 [32,33], are also fabricated and used for piezo-catalysis.

To our knowledge, DFUS coupled with a piezo-catalyst, such as ZnO, has not been applied for microbial inactivation neither for water disinfection nor for SDT. In our previous work, a high synergistic effect of DFUS (120 + 1700 kHz) coupled with persulfate was found for bacterial inactivation in water [34]. The choice of these frequencies is due to the wide use and low price of commercial converters and producers that make them attractive for full-scale application. Specifically, the first frequency (120 kHz) is applied for the precision cleaning of complicated industrial parts, and the second frequency (1700 kHz) is commonly used for making water mist in nebulizers and humidifying the indoor air.

The present study is the first to explore a potential synergy of high-frequency DFUS in the presence of persulfate and ZnO nano- and microparticles towards the piezo-catalytic inactivation of *Escherichia coli* and *Enterococcus faecalis* in synthetic water. The comparison of the piezo-catalytic performance of nano- and microparticles represents considerable interest due to their different toxicological properties. Furthermore, a novel hybrid system, which simultaneously exploits DFUS, ZnO and persulfate, was also examined for enhanced inactivation efficiency.

2. Materials and Methods

2.1. Test Bacteria

Bacterial strains *Enterococcus faecalis* B 4053 and *Escherichia coli* K-12 were supplied by the State Research Institute of Genetics and Selection of Industrial Microorganisms (Genetika, Moscow, Russia). Cultures of *E. faecalis* and *E. coli* were grown aerobically with shaking at 37 °C and 180 rpm (Biosan ES-20, Riga, Latvia) in tryptic soy broth (Merck, Darmstadt, Germany) and nutrient broth (SRCAMB, Obolensk, Russia), respectively. After

overnight culturing, the cells were harvested by centrifugation at 1690× *g* for 5 min (C2006, Centurion Scientific, Chichester, West Sussex, UK) and washed twice with phosphate-buffered saline (PBS, pH 7.4, Rosmedbio Ltd., St. Petersburg, Russia). Washed cells were then resuspended in PBS to obtain a stock suspension containing approximately 10^8 CFU/mL. For disinfection experiments, 1.5 L deionized water was contaminated with a 150 µL aliquot of cell suspension to obtain synthetic water with an initial cell count of 10^5 CFU/mL.

2.2. Single- and Dual-Frequency Ultrasonication

Inactivation experiments were performed in an orthogonal rectangle-shaped ultrasonic setup (Figure 1). Briefly, it represents a 4 L stainless steel water reservoir with four 120 kHz converters (50 W each, Fan Ying Sonic, Granbosonic Ultrasonic Producer 300 W/120 kHz, Shenzhen, China) on its long opposite sides and six 1700 kHz converters (total power 150 W, MSX, model ZCX-RM6D48F, Jiaxing, China) as a single unit, which was placed on the bottom of the reservoir. The water to be disinfected was thermostated at 20 ± 2 °C by a water jacket.

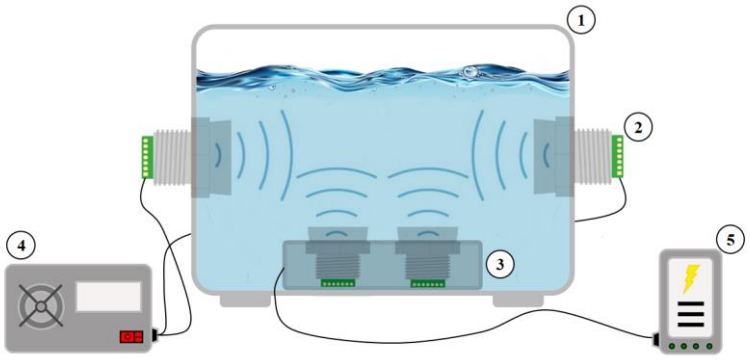

Figure 1. A diagram of dual-frequency ultrasonic setup. 1—water reservoir, 2—ceramic converter (120 kHz), 3—ceramic converter unit (1700 kHz), 4—ultrasonic producer (120 kHz), 5—power source (48 V).

Synthetic water containing 10^5 CFU/mL of *E. coli* or *E. faecalis* was irradiated in dual-frequency mode with added 1 g/L ZnO nano- or microparticles (99.7%, Hebei Shengyin Packaging Material Co., Ltd., Shijiazhuang, China) and 100 mg/L potassium persulfate (Vekton, St. Petersburg, Russia). Micro- and nanoparticles were 1 µm and 50 nm in size, respectively. Generally, the following hybrid systems were designed in this study:

- 120/1700 kHz/ZnO (50 nm);
- 120/1700 kHz/ZnO (1 µm);
- 120/1700 kHz/ZnO (50 nm)/$S_2O_8^{2-}$;
- 120/1700 kHz/ZnO (1 µm)/$S_2O_8^{2-}$.

To evaluate the synergistic effect of DFUS in terms of inactivation, target bacteria were also sequentially treated via single-frequency at 120 and 1700 kHz in the above piezocatalytic systems. The CFUs were enumerated via the serial dilution technique in triplicate after incubation on tryptic soy agar (*E. faecalis*) and nutrient agar (*E. coli*) plates at 37 °C for 24 h. The obtained data were presented as plots of the log reduction ($Lg(N/N_0)$) versus irradiation time (min). Each data point is the mean value (±SD) from 3 to 5 replicates. The statistical treatment of the data was carried out with the Statistica 10.0 software program.

Radical scavenging tests were conducted under DFUS conditions using *p*-chlorobenzoic acid (*p*CBA) as a probe compound (Supplementary Material, Text S1).

3. Results and Discussion

3.1. Single-Frequency Piezo-Catalytic Inactivation

The efficiency of single-frequency inactivation was compared in terms of log reduction between two frequencies (120 and 1700 kHz), ZnO- and $S_2O_8^{2-}$-mediated processes and ZnO particle sizes (50 nm and 1 µm). The target bacteria were resistant to ultrasonic exposure at 120 or 1700 kHz alone, while adding an oxidant or catalyst caused a measurable inactivation in most cases. Comparing two frequencies, 1700 kHz performed better than 120 kHz in the presence of ZnO or $S_2O_8^{2-}$ (1700 kHz/ZnO and 1700 kHz/$S_2O_8^{2-}$ systems), and 5-log (total) reduction was attained with this frequency and persulfate (Figure 2).

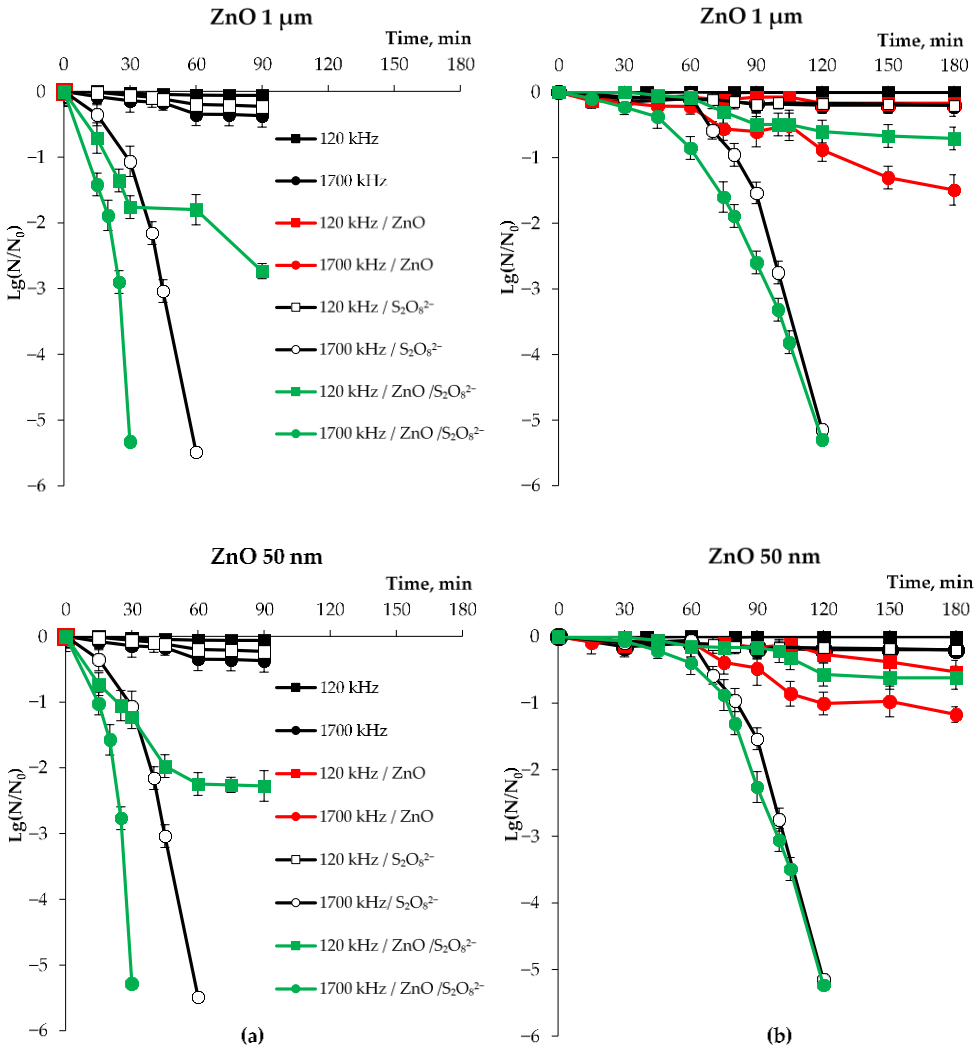

Figure 2. Single-frequency piezo-catalytic inactivation of *E. coli* (**a**) and *E. faecalis* (**b**) in the presence of ZnO micro- and nanoparticles and persulfate. $N_0 = 10^5$ CFU/mL, $[ZnO]_0 = 1$ g/L, $[S_2O_8^{2-}]_0 = 0.1$ g/L. Error bars represent ±SD.

The obtained result suggests that more ROS are produced under ZnO or $S_2O_8^{2-}$ activation with 1700 kHz. This is consistent with the data of Vighetto et al. (2019) [35], who found that ROS exposure at 1 MHz in the presence of ZnO-NH_2 nanocrystals (20 nm) was one order of magnitude higher than that obtained at 150 kHz. The authors proposed that the applied ultrasonic conditions were even sufficient to initiate the acoustic cavitation of gas nanobubbles trapped at the catalyst surface. Earlier, Mason et al. (2011) [36] proved that the efficiency of •OH production increases as the frequency is increased and more radical reactions occur at higher frequencies. This is explained by decreasing the radius of microbubbles with increasing frequency, which accelerates their collapse and yields

more ROS. Particularly, the microbubble radius at 500 kHz was ~25-fold lower than that measured at 20 kHz, and higher production of H_2O_2 and •OH was observed [37].

Under dark conditions, i.e., upon contact of cells with ZnO micro- and nanoparticles without ultrasonic exposure, *E. coli* was reduced by ~1-log and *E. faecalis* was not inactivated (Supplementary Material, Figure S1). In 120 kHz/ZnO mode, *E. faecalis* remained resistant, whereas *E. coli* was inactivated by 1.8–1.9-log at both particle sizes. Considering the 1700 kHz/ZnO process, the log reduction of *E. coli* with 1 µm ZnO was significantly higher than that observed with 50 nm (4.3-log vs. 2.6-log after 90 min exposure). Meanwhile, this finding was not significant for *E. faecalis* (1.5-log vs. 1.2-log after 180 min exposure). It is known that ZnO toxicity increases with decreasing the particle size and ZnO nanoparticles are more toxic to bacteria than microparticles [38]. Furthermore, ZnO nanoparticles were reported to be the most toxic to different bacteria among the nano-sized TiO_2, Al_2O_3 and SiO_2 [39]. However, piezo-catalytic inactivation in the absence of persulfate appears to have an inverse relationship, and the microparticles make a greater contribution to ROS generation. This is supported by the fact that the piezoelectric properties of ZnO microparticles (~10 µm) are significantly higher than those of nanoparticles (80–100 nm) [40]. It is known that piezoelectric properties are quantitatively described by the piezoelectric coefficient (usually written "d_{33}"). Li et al. (2015) [41] found that d_{33} depends on the ZnO particle size, increasing from 8.36 pm/V at 800 nm to 46.97 pm/V at 1.5 µm. Accordingly, the piezoelectric properties of ZnO microparticles are several times superior to nanoparticles, and therefore the former generates more radicals.

The comparison of the 1700 kHz/$S_2O_8^{2-}$ and 1700 kHz/ZnO modes showed the higher efficiency of the persulfate-based process by which *E. coli* and *E. faecalis* were completely inactivated after 60 and 120 min exposure, respectively. In all cases, the inactivation of *E. faecalis*, which is the more resistant Gram-positive bacterium, required prolonged irradiation time as compared to *E. coli*. The hybrid system {1700 kHz/ZnO/$S_2O_8^{2-}$} was the most efficient for eradicating *E. coli* by 5-log for 30 min treatment (Figure 2). On the contrary, the performance of this system for the total inactivation of *E. faecalis* was similar to that of the 1700 kHz/$S_2O_8^{2-}$ process. Notably, when using 1 µm ZnO, the lag period was shorter and the log reduction was higher up to 90 min exposure.

The hybrid system {120 kHz/ZnO/$S_2O_8^{2-}$} was much less efficient and showed on average a 2.5- and about a 1-log reduction in *E. coli* (90 min) and *E. faecalis* (180 min), respectively. No effect of particle size was observed when comparing the performance of hybrid US/ZnO/$S_2O_8^{2-}$ processes, presumably due to the dominating effect of activated persulfate. This can be explained by the greater yield of ROS (SO_4•$^-$ and •OH) from activated persulfate as compared to ZnO (•OH). Wen et al. (2023) [42] also reported that SO_4•$^-$ and •OH (as a product of SO_4•$^-$ hydrolysis) were produced under the piezo-activation of Co-ZnO nanorods and persulfate.

In summary, single-frequency experiments revealed that piezo-catalytic inactivation with 1700 kHz was more efficient than that with 120 kHz. The performance of 1700 kHz-based processes can be ranked for *E. coli* as follows: 1700 kHz < 1700 kHz/ZnO < 1700 kHz/$S_2O_8^{2-}$ < 1700 kHz/ZnO/$S_2O_8^{2-}$. For *E. faecalis*, the 1700 kHz/$S_2O_8^{2-}$ process performed comparably in the absence and presence of ZnO that assumes the hidden contribution of the catalyst.

3.2. Dual-Frequency Piezo-Catalytic Inactivation and Synergistic Effect

Figure 3 shows that DFUS alone can slightly inactivate selected bacteria. Specifically, *E. coli* was inactivated by 1.7-log, whereas *E. faecalis* did not exhibit measurable inactivation after 90 min exposure. To enhance the generation of ROS and explore the potential synergistic effect between two frequencies, dual-frequency piezo-catalytic inactivation was investigated using ZnO particles and persulfate separately and simultaneously. As can be seen from Figure 3, the hybrid system {120/1700 kHz/ZnO/$S_2O_8^{2-}$} provided the fastest total inactivation of *E. coli* (25 min).

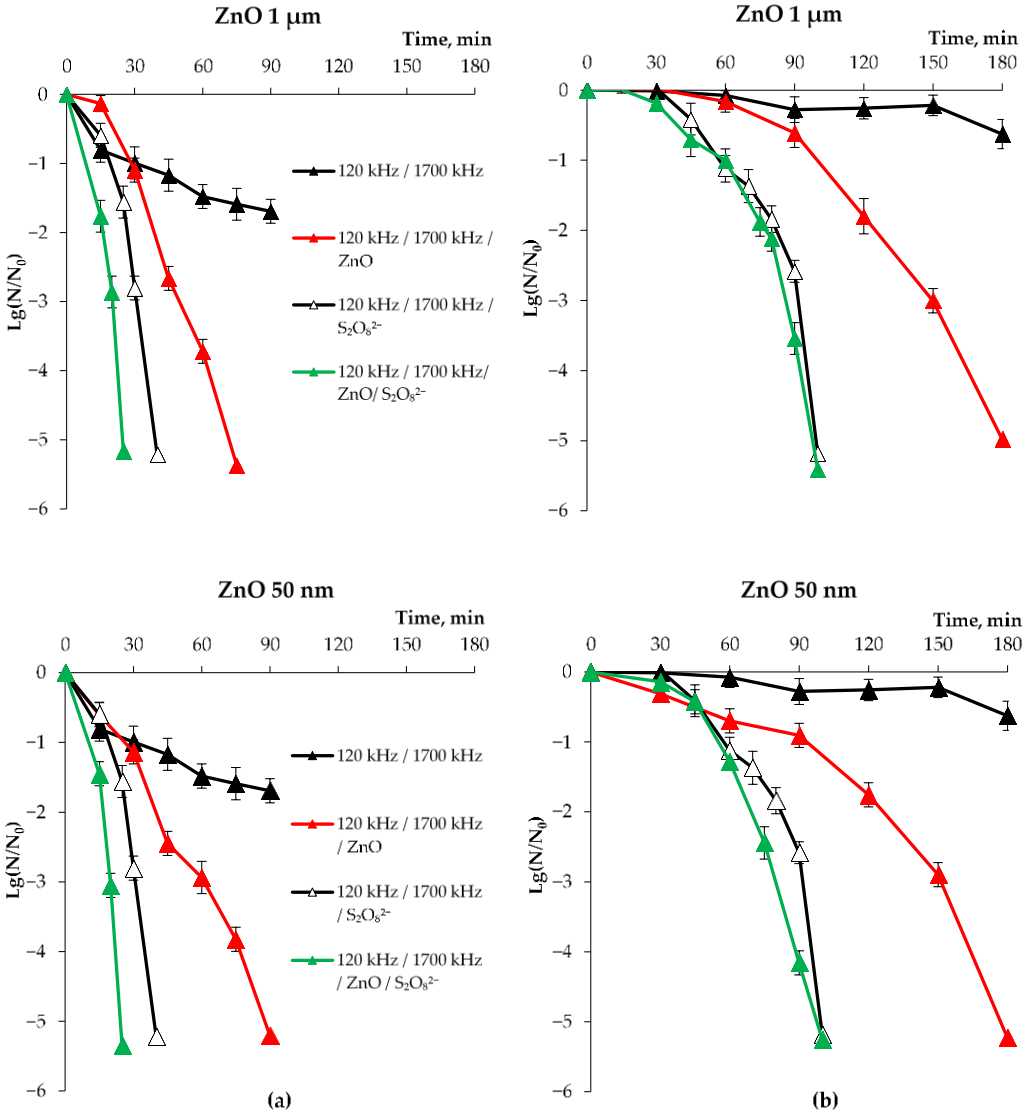

Figure 3. Dual-frequency piezo-catalytic inactivation of *E. coli* (**a**) and *E. faecalis* (**b**) in the presence of ZnO micro- and nanoparticles and persulfate. N_0 = 10^5 CFU/mL, $[ZnO]_0$ = 1 g/L, $[S_2O_8{}^{2-}]_0$ = 0.1 g/L. Error bars represent ±SD.

Similar to single-frequency disinfection, the inactivation kinetics of *E. faecalis* via the DFUS/$S_2O_8{}^{2-}$/ZnO and DFUS/$S_2O_8{}^{2-}$ processes were similar, and a 5-log reduction was achieved after the same exposure time (100 min). In turn, the DFUS/$S_2O_8{}^{2-}$ process was also more efficient than the DFUS/ZnO process and the difference was more pronounced for *E. faecalis*. As observed under single-frequency ZnO/$S_2O_8{}^{2-}$ conditions, no difference between the 50 nm and 1 µm particle sizes was found in the {DFUS/ZnO/$S_2O_8{}^{2-}$} system. In the absence of persulfate (DFUS/ZnO), the performance of 1 µm for inactivating *E. coli* was also higher than that observed with 50 nm. Specifically, the complete (5-log) inactivation of *E. coli* was attained faster using ZnO microparticles. No effect of particle size was observed for *E. faecalis*, and its 5-log reduction required the same time (180 min) (Figure 3).

The synergistic effect of DFUS in efficient systems was evaluated through the synergistic coefficient (SC). An SC value larger than 1 indicates synergy, whereas an additive and an antagonistic effect are observed when the SC is equal to and less than 1, respectively [6]. A synergy occurs if log reduction after DFUS treatment is higher than the sum of log reductions obtained after single-frequency treatment. The log reductions in single-frequency mode were obtained for the same exposure periods, which were needed for achieving a 5-log reduction in DFUS mode (Table 1). A fixed time for evaluating a synergy of DFUS

was also previously used by Adelnia et al. (2020) [43]. Given that approach, the synergistic coefficient was determined relative to the 5-log reduction times for the DFUS process (1):

$$SC = \frac{\text{Log reduction}(120 + 1700\ \text{kHz})}{\text{Log reduction}(120\ \text{kHz}) + \text{Log reduction}(1700\ \text{kHz})} \quad (1)$$

Table 1. The synergistic coefficients of piezo-catalytic inactivation using DFUS (120 + 1700 kHz), ZnO particles and persulfate.

Strain	System	ZnO Particle Size	5-Log Reduction Time, min	Sum of Log Reductions after Single-Frequency Treatment	SC
E. coli K-12	DFUS/ZnO/$S_2O_8^{2-}$	50 nm	25	3.8	1.3
		1 µm	25	4.3	1.2
	DFUS/ZnO	50 nm	90	4.4	1.2
		1 µm	75	4.4	1.2
	DFUS/$S_2O_8^{2-}$	no ZnO	40	2.3	2.3
E. faecalis B 4053	DFUS/ZnO/$S_2O_8^{2-}$	50 nm	100	3.3	1.5
		1 µm	100	3.8	1.4
	DFUS/ZnO	50 nm	180	1.7	3.0
		1 µm	180	1.7	2.9
	DFUS/$S_2O_8^{2-}$	no ZnO	100	2.9	1.8

Generally, the synergistic effect for inactivating *E. faecalis* by ZnO-based processes was higher than that for *E. coli*, which is a more susceptible organism and inactivated faster (Table 1). Interestingly, SC values were similar for micro- and nanoparticles within the same system. In the case of the DFUS/$S_2O_8^{2-}$ process, *E. coli* exhibited higher synergy due to a greater difference between dual- and single-frequency (1700 kHz/$S_2O_8^{2-}$) inactivation curves (Supplementary Material, Figure S2). The highest synergistic effect (SC = 3.0) was found for *E. faecalis* in the {DFUS/ZnO} system (Supplementary Material, Figure S3), whereas the SC value for *E. coli* was lower by a factor of 2.5. This is explained by the contribution of the 120 kHz/ZnO system (1.8–1.9 log reduction), which reduced the synergistic effect of the DFUS mode for *E. coli* (Supplementary Material, Figure S2).

It is known that the dual-frequency ultrasonication of water enhances acoustic cavitation due to the production of new (combination) frequencies, as discussed in detail previously [6,44]. Briefly, under the nonlinear interaction of two acoustic waves at different frequencies in water, the combination frequencies are produced alongside the main and additional frequencies (harmonics, subharmonics, and ultraharmonics). The combination frequencies represent a sum or a difference of two main frequencies, main frequencies, harmonics and so on. These new frequencies make the oscillating microbubbles unstable and increase the probability of their collapse [45], which enhances cavitation and generates more ROS. Specifically, Lei et al. (2020) [46] explored the system {20 + 43 kHz/persulfate} towards the degradation of petroleum hydrocarbons and confirmed that DFUS generates more $SO_4\bullet^-$ and •OH than single-frequency US/persulfate.

A synergistic effect can be attributed to the boosted generation of ROS, thus intensifying the inactivation processes. The increased generation of •OH and $SO_4\bullet^-$ was also reported under the activation of persulfate with low-frequency DFUS for the synergistic degradation of per- and polyfluoroalkyl substances [47]. Other related research dealt with the single-frequency system {US/ZnO/$S_2O_8^{2-}$}, which has attracted attention for its cost efficiency. This system was majorly induced by •OH and $SO_4\bullet^-$ [48,49]; other ROS, such as $^1O_2$ and $\bullet O_2^-$, were also identified [42,50,51]. These ROS destroy the cellular membrane by damaging proteins and lipids. The examination of the cell wall of *E. coli* by scanning electron microscopy (SEM) showed its disruption after exposure to •OH from US/ZnO [52]. Our •OH scavenging tests showed that *p*CBA was degraded faster by the {120 + 1700 kHz/ZnO/$S_2O_8^{2-}$} process as compared to the {120 + 1700 kHz} process

(Supplementary Material, Figure S4). This indicates that more ROS were produced in the presence of ZnO and persulfate.

We propose that cell permeabilization via acoustic cavitation (sonoporation) also plays an important role in inactivation. Zhang et al. (2012) [53] investigated different types of sonoporation in detail using SEM and found that the morphological changes of the cell wall and its poration were lethal to cells. Recently, Ali et al. (2023) [54] reviewed the data on exposure to ROS and ultrasound and reported that the radicals were also produced inside the cell (intracellular ROS). Sonoporation facilitates the penetration of ZnO particles [15] and extracellular ROS (generated outside the cell) into sonoporated cells [3] that ultimately accelerate their apoptosis. In turn, the penetrated ZnO particles also generate intracellular ROS which damage the organelles [15].

In summary, a synergistic effect of DFUS in the presence of ZnO and $S_2O_8^{2-}$ is supposed to be driven by the simultaneous action of two different mechanisms of inactivation via (1) generated ROS and (2) sonoporation with associated effects. A comparison of DFUS-based processes showed that the contribution of ZnO was also hidden in the DFUS/ZnO/$S_2O_8^{2-}$ process for *E. faecalis*. For *E. coli*, the efficiency of DFUS-based processes increased in the order: DFUS < DFUS/ZnO < DFUS/$S_2O_8^{2-}$ < DFUS/ZnO/$S_2O_8^{2-}$.

4. Conclusions

This study revealed the synergistic inactivation of *E. coli* and *E. faecalis* in synthetic water via dual-frequency ultrasound at 120 and 1700 kHz with added persulfate and ZnO particles. Apparently, the intensification of inactivation processes under DFUS exposure is driven by at least two key processes, attack by increased ROS yield and sonoporation, which ultimately create a synergistic effect. Microparticles, which are more favorable to the aquatic environment, were found to be more efficient than nanoparticles for inactivating *E. coli* via ZnO-mediated processes. The present study supplies the integration of high-frequency DFUS, persulfate and piezo-catalyst ZnO as a novel approach for further development in water disinfection.

Supplementary Materials: The following supporting information can be downloaded at: https://www.mdpi.com/article/10.3390/w15162937/s1, Figure S1: Inactivation of bacteria in the presence of ZnO micro- and nanoparticles under dark conditions (control); Figure S2: Single- and dual-frequency inactivation of *E. coli* in the presence of ZnO micro- and nanoparticles and persulfate; Figure S3: Single- and dual-frequency inactivation of *E. faecalis* in the presence of ZnO micro- and nanoparticles and persulfate; Figure S4: Dual-frequency degradation of *p*CBA in the absence and presence of ZnO microparticles and persulfate.

Author Contributions: Investigation, validation, formal analysis, I.T. and E.K.; writing—original draft preparation, data curation, G.M.; writing—review and editing, project administration, conceptualization, methodology, supervision, V.B. All authors have read and agreed to the published version of the manuscript.

Funding: This research was funded by Russian Science Foundation, grant number 22-24-00482.

Data Availability Statement: Data is contained within the article and Supplementary Material.

Conflicts of Interest: The authors declare no conflict of interest.

References

1. Sathishkumar, P.; Mangalaraja, R.V.; Anandan, S. Review on the recent improvements in sonochemical and combined sonochemical oxidation processes—A powerful tool for destruction of environmental contaminants. *Ren. Sustain. Energy Rev.* **2016**, *55*, 426–454. [CrossRef]
2. Ince, N.H. Ultrasound-assisted advanced oxidation processes for water decontamination. *Ultrason. Sonochem.* **2018**, *40*, 97–103. [CrossRef]
3. Matafonova, G.; Batoev, V. Review on low- and high-frequency sonolytic, sonophotolytic and sonophotochemical processes for inactivating pathogenic microorganisms in aqueous media. *Water Res.* **2019**, *166*, 115085. [CrossRef]
4. Yap, H.C.; Pang, Y.L.; Lim, S.; Abdullah, A.Z.; Ong, H.C.; Wu, C.-H. A comprehensive review on state-of-the-art photo-, sono-, and sonophotocatalytic treatments to degrade emerging contaminants. *Int. J. Environ. Sci. Technol.* **2019**, *16*, 601–628. [CrossRef]

5. Dehghani, M.H.; Karri, R.R.; Koduru, J.R.; Manickam, S.; Tyagi, I.; Mubarak, N.M. Recent trends in the applications of sonochemical reactors as an advanced oxidation process for the remediation of microbial hazards associated with water and wastewater: A critical review. *Ultrason. Sonochem.* **2023**, *94*, 106302. [CrossRef] [PubMed]
6. Matafonova, G.; Batoev, V. Dual-frequency ultrasound: Strengths and shortcomings to water treatment and disinfection. *Water Res.* **2020**, *182*, 116016. [CrossRef] [PubMed]
7. Wu, X.; Mason, T.J. Evaluation of power ultrasonic effects on algae cells at a small pilot scale. *Water* **2017**, *9*, 470. [CrossRef]
8. Zou, H.; Tang, H. Comparison of different bacteria inactivation by a novel continuous-flow ultrasound/chlorination water treatment system in a pilot scale. *Water* **2019**, *11*, 258. [CrossRef]
9. Zou, H.; Wang, L. The disinfection effect of a novel continuous-flow water sterilizing system coupling dual-frequency ultrasound with sodium hypochlorite in pilot scale. *Ultrason. Sonochem.* **2017**, *36*, 246–252. [CrossRef]
10. Alamolhoda, M.; Mokhtari-Dizaji, M.; Barati, A.H.; Hasanzadeh, H. Comparing the in vivo sonodynamic effects of dual- and single-frequency ultrasound in breast adenocarcinoma. *J. Med. Ultrason.* **2012**, *39*, 115–125. [CrossRef] [PubMed]
11. Serpe, L.; Giuntini, F. Sonodynamic antimicrobial chemotherapy: First steps towards a sound approach for microbe inactivation. *J. Photochem. Photobiol. B* **2015**, *150*, 44–49. [CrossRef] [PubMed]
12. Rengeng, L.; Qianyu, Z.; Yuehong, L.; Zhongzhong, P.; Libo, L. Sonodynamic therapy, a treatment developing from photodynamic therapy. *Photodiagnosis Photodyn. Ther.* **2017**, *19*, 159–166. [CrossRef] [PubMed]
13. Tabatabaei, Z.S.; Rajabi, O.; Nassirli, H.; Noghreiyan, A.V.; Sazgarnia, A. A comparative study on generating hydroxyl radicals by single and two-frequency ultrasound with gold nanoparticles and protoporphyrin IX. *Australas. Phys. Eng. Sci. Med.* **2019**, *42*, 1039–1047. [CrossRef] [PubMed]
14. Fan, L.; Muhammad, A.I.; Ismail, B.B.; Liu, D. Sonodynamic antimicrobial chemotherapy: An emerging alternative strategy for microbial inactivation. *Ultrason. Sonochem.* **2021**, *75*, 105591. [CrossRef] [PubMed]
15. Zhang, L.; Qi, H.; Yan, Z.; Gu, Y.; Sun, W.; Zewde, A.A. Sonophotocatalytic inactivation of *E. coli* using ZnO nanofluids and its mechanism. *Ultrason. Sonochem.* **2017**, *34*, 232–238. [CrossRef] [PubMed]
16. Bayrami, A.; Alioghli, S.; Rahim Pouran, S.; Habibi-Yangjeh, A.; Khataee, A.; Ramesh, S. A facile ultrasonic-aided biosynthesis of ZnO nanoparticles using *Vaccinium arctostaphylos* L. leaf extract and its antidiabetic, antibacterial, and oxidative activity evaluation. *Ultrason. Sonochem.* **2019**, *55*, 57–66. [CrossRef]
17. Wang, G.; Wu, W.; Zhu, J.-J.; Peng, D. The promise of low-intensity ultrasound: A review on sonosensitizers and sonocatalysts by ultrasonic activation for bacterial killing. *Ultrason. Sonochem.* **2021**, *79*, 105781. [CrossRef]
18. Su, K.; Tan, L.; Liu, X.; Cui, Z.; Zheng, Y.; Li, B.; Han, Y.; Li, Z.; Zhu, S.; Liang, Y.; et al. Rapid photo-sonotherapy for clinical treatment of bacterial infected bone implants by creating oxygen deficiency using sulfur doping. *ACS Nano* **2020**, *14*, 2077–2089. [CrossRef]
19. Wang, Y.; Sun, Y.; Liu, S.; Zhi, L.; Wang, X. Preparation of sonoactivated TiO_2-DVDMS nanocomposite for enhanced antibacterial activity. *Ultrason. Sonochem.* **2020**, *63*, 104968. [CrossRef]
20. Pourhajibagher, M.; Bahador, A. Synergistic biocidal effects of metal oxide nanoparticles-assisted ultrasound irradiation: Antimicrobial sonodynamic therapy against *Streptococcus mutans* biofilms. *Photodiagnosis Photodyn. Ther.* **2021**, *35*, 102432. [CrossRef]
21. Wu, M.; Zhang, Z.; Liu, Z.; Zhang, J.; Zhang, Y.; Ding, Y.; Huang, T.; Xiang, D.; Wang, Z.; Dai, Y.; et al. Piezoelectric nanocomposites for sonodynamic bacterial elimination and wound healing. *Nano Today* **2021**, *37*, 101104. [CrossRef]
22. Xu, Q.; Xiu, W.; Li, Q.; Zhang, Y.; Li, X.; Ding, M.; Yang, D.; Mou, Y.; Dong, H. Emerging nanosonosensitizers augment sonodynamic-mediated antimicrobial therapies. *Mater. Today Bio* **2023**, *19*, 100559. [CrossRef] [PubMed]
23. Ninomiya, K.; Noda, K.; Ogino, C.; Kuroda, S.; Shimizu, N. Enhanced OH radical generation by dual-frequency ultrasound with TiO_2 nanoparticles: Its application to targeted sonodynamic therapy. *Ultrason. Sonochem.* **2014**, *21*, 289–294. [CrossRef] [PubMed]
24. Wang, Z.L.; Song, J. Piezoelectric nanogenerators based on zinc oxide nanowire arrays. *Science* **2006**, *312*, 242–246. [CrossRef]
25. Jiang, Z.; Tan, X.; Huang, Y. Piezoelectric effect enhanced photocatalysis in environmental remediation: State-of-the-art techniques and future scenarios. *Sci. Tot. Environ.* **2022**, *806*, 150924. [CrossRef]
26. Ma, W.; Lv, M.; Cao, F.; Fang, Z.; Feng, Y.; Zhang, G.; Yang, Y.; Liu, H. Synthesis and characterization of ZnO-GO composites with their piezoelectric catalytic and antibacterial properties. *J. Environ. Chem. Eng.* **2022**, *10*, 107840. [CrossRef]
27. Kumar, S.; Sharma, M.; Frömling, T.; Vaish, R. Antibacterial ferroelectric materials: Advancements and future directions. *J. Ind. Eng. Chem.* **2021**, *97*, 95–110. [CrossRef]
28. Zhao, Y.; Low, Z.-X.; Pan, Y.; Zhong, Z.; Gao, G. Universal water disinfection by piezoelectret aluminium oxide-based electroporation and generation of reactive oxygen species. *Nano Energy* **2021**, *92*, 106749. [CrossRef]
29. Li, J.; Liu, X.; Zhao, G.; Liu, Z.; Cai, Y.; Wang, S.; Shen, C.; Hu, B.; Wang, X. Piezoelectric materials and techniques for environmental pollution remediation. *Sci. Total Environ.* **2023**, *869*, 161767. [CrossRef]
30. Daraei, H.; Maleki, A.; Mahvi, A.H.; Zandsalimi, Y.; Alaei, L.; Gharibi, F. Synthesis of ZnO nano-sono-catalyst for degradation of reactive dye focusing on energy consumption: Operational parameters influence, modeling, and optimization. *Desalin. Water Treat.* **2014**, *52*, 6745–6755. [CrossRef]
31. Tamboia, G.; Campanini, M.; Vighetto, V.; Racca, L.; Spigarelli, L.; Canavese, G.; Cauda, V. A comparative analysis of low intensity ultrasound effects on living cells: From simulation to experiments. *Biomed. Microdev.* **2022**, *24*, 35. [CrossRef] [PubMed]
32. Porwal, C.; Verma, S.; Chauhan, S.V.; Vaish, R. Bismuth zinc borate- Polyacrylonitrile nanofibers for photo-piezocatalysis. *J. Ind. Eng. Chem.* **2023**, *124*, 358–367. [CrossRef]

33. Porwal, C.; Sharma, M.; Vaish, R.; Chauhan, V.S.; ben Ahmed, S.; Hwang, W.; Park, H.K.B.; Sung, T.H.; Kumar, A. Piezocatalytic dye degradation using Bi_2O_3-ZnO-B_2O_3 glass-nanocomposites. *J. Mater. Res. Technol.* **2022**, *21*, 2028–2037. [CrossRef]
34. Garkusheva, N.; Tsenter, I.; Kobunova, E.; Matafonova, G.; Batoev, V. Dual-frequency ultrasonic inactivation of *Escherichia coli* and *Enterococcus faecalis* using persulfate: A synergistic effect. *Water* **2022**, *14*, 2604. [CrossRef]
35. Vighetto, V.; Ancona, A.; Racca, L.; Limongi, T.; Troia, A.; Canavese, G.; Cauda, V. The synergistic effect of nanocrystals combined with ultrasound in the generation of reactive oxygen species for biomedical applications. *Front. Bioeng. Biotechnol.* **2019**, *7*, 374. [CrossRef]
36. Mason, T.J.; Cobley, A.J.; Graves, J.E.; Morgan, D. New evidence for the inverse dependence of mechanical and chemical effects on the frequency of ultrasound. *Ultrason. Sonochem.* **2011**, *18*, 226–230. [CrossRef]
37. Hua, I.; Hoffmann, M.R. Optimization of ultrasonic irradiation as an advanced oxidation technology. *Environ. Sci. Technol.* **1997**, *31*, 2237–2243. [CrossRef]
38. Ann, L.C.; Mahmud, S.; Seeni, A.; Bakhori, S.K.M.; Sirelkhatim, A.; Mohamad, D.; Hasan, H. Structural morphology and in vitro toxicity studies of nano- and micro-sized zinc oxide structures. *J. Environ. Chem. Eng.* **2015**, *3*, 436–444. [CrossRef]
39. Jiang, W.; Mashayekhi, H.; Xing, B. Bacterial toxicity comparison between nano- and micro-scaled oxide particles. *Environ. Pollut.* **2009**, *157*, 1619–1625. [CrossRef]
40. Zhang, X.; Le, M.-Q.; Zahhaf, O.; Capsal, J.-F.; Cottinet, P.-J.; Petit, L. Enhancing dielectric and piezoelectric properties of micro-ZnO/PDMS composite-based dielectrophoresis. *Mater. Des.* **2020**, *192*, 108783. [CrossRef]
41. Li, T.; Li, Y.T.; Qin, W.W.; Zhang, P.P.; Chen, X.Q.; Hu, X.F.; Zhang, W. Piezoelectric size effects in a zinc oxide micropillar. *Nanoscale Res. Lett.* **2015**, *10*, 394. [CrossRef] [PubMed]
42. Wen, Y.; Chen, J.; Gao, X.; Liu, W.; Che, H.; Liu, B.; Ao, Y. Two birds with one stone: Cobalt-doping induces to enhanced piezoelectric property and persulfate activation ability of ZnO nanorods for efficient water purification. *Nano Energy* **2023**, *107*, 108173. [CrossRef]
43. Adelnia, A.; Mokhtari-Dizaji, M.; Hoseinkhani, S.; Bakhshandeh, M. The effect of dual-frequency ultrasound waves on B16F10 melanoma cells: Sonodynamic therapy using nanoliposomes containing methylene blue. *Skin Res. Technol.* **2021**, *27*, 376–384. [CrossRef]
44. Zhang, Y.; Zhang, Y.; Li, S. Combination and simultaneous resonances of gas bubbles oscillating in liquids under dual-frequency acoustic excitation. *Ultrason. Sonochem.* **2017**, *35*, 431–439. [CrossRef]
45. Ye, L.; Zhu, X.; Liu, Y. Numerical study on dual-frequency ultrasonic enhancing cavitation effect based on bubble dynamic evolution. *Ultrason. Sonochem.* **2019**, *59*, 104744. [CrossRef]
46. Lei, Y.-J.; Zhang, J.; Tian, Y.; Yao, J.; Duan, O.-S.; Zuo, F. Enhanced degradation of total petroleum hydrocarbons in real soil by dual-frequency ultrasound-activated persulfate. *Sci. Tot. Environ.* **2020**, *748*, 141414. [CrossRef]
47. Lei, Y.-J.; Tian, Y.; Sobhani, Z.; Naidu, R.; Fang, C. Synergistic degradation of PFAS in water and soil by dual-frequency ultrasonic activated persulfate. *Chem. Eng. J.* **2020**, *388*, 124215. [CrossRef]
48. Hu, S.-B.; Li, L.; Luo, M.-Y.; Yun, Y.-F.; Chang, C.-T. Aqueous norfloxacin sonocatalytic degradation with multilayer flower-like ZnO in the presence of peroxydisulfate. *Ultrason. Sonochem.* **2017**, *38*, 446–454. [CrossRef] [PubMed]
49. Liu, F.; Yi, P.; Wang, X.; Gao, H.; Zhang, H. Degradation of Acid Orange 7 by an ultrasound/ZnO-GAC/persulfate process. *Sep. Pur. Technol.* **2018**, *194*, 181–187. [CrossRef]
50. Subramani, A.K.; Rani, P.; Wang, P.-H.; Chen, B.-Y.; Mohan, S.; Chang, C.-T. Performance assessment of the combined treatment for oxytetracycline antibiotics removal by sonocatalysis and degradation using *Pseudomonas aeruginosa*. *J. Environ. Chem. Eng.* **2019**, *7*, 103215. [CrossRef]
51. Zhang, M.; Tao, H.; Zhai, C.; Yang, J.; Zhou, Y.; Xia, D.; Comodi, G.; Zhu, M. Twin-brush ZnO mesocrystal for the piezo-activation of peroxymonosulfate to remove ibuprofen in water: Performance and mechanism. *Appl. Catal. B* **2023**, *326*, 122399. [CrossRef]
52. Anju, S.G.; Bright Singh, I.S.; Yesodharan, E.P.; Yesodharan, S. Investigations on semiconductor sonocatalysis for the removal of pathological micro-organisms in water. *Desalin. Water Treat.* **2015**, *54*, 3161–3168. [CrossRef]
53. Zhang, J.-Z.; Saggar, J.K.; Zhou, Z.-L.; Hu, B. Different effects of sonoporation on cell morphology and viability. *Bosn. J. Basic Med. Sci.* **2012**, *12*, 64–68. [CrossRef] [PubMed]
54. Ali, A.; Chen, L.; Nasir, M.S.; Wu, C.; Guo, B.; Yang, Y. Piezocatalytic removal of water bacteria and organic compounds: A review. *Environ. Chem. Lett.* **2023**, *21*, 1075–1092. [CrossRef]